NUMERICAL ANALYSIS OF THE SELF-SUSTAINING TRAVELING WAVE OF NUCLEAR FISSION PROPAGATED BY EPITHERMAL NEUTRONS IN URANIUM DICARBIDE MEDIUM

Article *in* Nuclear Physics and Atomic Energy · January 2024

DOI: 10.15407/jnpae2024.04.357

CITATIONS
0

READS
18

5 authors, including:

Sergey A. Chernegenko
Odessa National Polytechnic University
34 PUBLICATIONS **132** CITATIONS
SEE PROFILE

Victor Tarasov
Odessa National Polytechnic University
59 PUBLICATIONS **233** CITATIONS
SEE PROFILE

АТОМНА ЕНЕРГЕТИКА
ATOMIC ENERGY

УДК 621.039.5 https://doi.org/10.15407/jnpae2024.04.357

M. R. Shcherbyna*, K. O. Shcherbyna, V. O. Tarasov, S. I. Kosenko, S. A. Chernezhenko

Odesa Polytechnic National University, Odesa, Ukraine

*Corresponding author: mykhailo.shcherbyna@yahoo.com

NUMERICAL ANALYSIS OF THE SELF-SUSTAINING TRAVELING WAVE OF NUCLEAR FISSION PROPAGATED BY EPITHERMAL NEUTRONS IN URANIUM DICARBIDE MEDIUM[1]

This study investigates the self-sustaining traveling wave of nuclear fission in a uranium dicarbide medium by numerically solving a system of partial differential equations. The primary focus is on the neutron diffusion equation and nuclide balance equations, which are crucial for understanding the behavior of fission waves. By solving these equations, we aim to determine the propagation characteristics and assess the stability of nuclear fission waves in uranium dicarbide. Numerical analysis provides significant insights into the dynamics of neutron distribution and nuclide evolution, enhancing our understanding of the underlying physical processes and their implications for traveling wave reactor design.

Keywords: traveling wave reactor, epithermal neutrons, uranium dicarbide, neutron diffusion equation, reactor design, self-sustaining fission wave.

1. Introduction

The traveling wave reactor (TWR) represents an advanced nuclear reactor design with significant advantages over traditional models. In a TWR, the nuclear reaction front progresses through the fuel material, converting fertile material into fissile material as it advances. One of the main advantages of this design is the inherent safety of these reactors. This concept also offers the promise of improved fuel utilization and reduced waste generation compared to conventional reactor designs. Furthermore, it may enable the use of unconventional fuels such as depleted uranium or thorium, which are abundant and currently considered waste products in nuclear fuel cycles.

Research on traveling wave regimes of nuclear fission in fissile reactor media, prior to 2013, was conducted exclusively in the realm of fast neutrons (e.g., [1 - 31]). This focus was due to the criterion for traveling wave propagation, formulated in [1], which is satisfied only for fast neutrons. However, fast neutrons impose harsh conditions (~500 DPA) on the structural materials and the fuel of such reactors [24 - 26], which cannot be met in the foreseeable future.

A solution to the issue of radiation resistance in TWRs was proposed in [32]. The criterion for traveling wave propagation was studied for uranium fuel across a broad energy spectrum of neutrons (0.001 eV - 1 MeV), and it was found that the criterion is satisfied not only in the fast neutron energy region but also in the epithermal range (1 - 7 eV). Furthermore, [32] presented the results of simplified 1D modeling, demonstrating the feasibility of a traveling wave of nuclear fission in natural uranium driven by epithermal neutrons. It was suggested that future research efforts should focus on this direction. However, since then, only five studies [33 - 37] have been published that report on traveling wave regimes in fissile reactor media using non-fast neutrons.

This study investigates the propagation of a traveling wave of nuclear fission within a cylindrical uranium dicarbide (UC_2) medium propagated by epithermal neutrons. UC_2 was selected for its effectiveness as a neutron moderator, facilitating the formation of the epithermal spectrum [38 - 39], as well as for its high thermal conductivity and robustness under high-temperature conditions. To initiate nuclear reactions, a neutron flux of 10^{15} $cm^{-2}s^{-1}$ was chosen. According to [40, 41], this neutron flux density is representative of operational pulsed nuclear reactors. Additionally, [42] notes that compact pulsed nuclear reactors with even higher neutron flux densities have already been developed.

2. Governing equations

The neutron diffusion equation defines neutron behavior. Mathematically, its general form in the one-group approximation is:

[1] Presented at the XXXI Annual Scientific Conference of the Institute for Nuclear Research of the National Academy of Sciences of Ukraine, Kyiv, May 27 - 31, 2024.

$$\frac{1}{v}\frac{\partial\phi(\vec{r},t)}{\partial t}=\nabla\left[D\left(\phi(\vec{r},t),\vec{r},t\right)\nabla\phi(\vec{r},t)\right]-$$

$$-\phi(\vec{r},t)\sum_m\Sigma_{a,m}(\vec{r},t)+S\left(\phi(\vec{r},t),\vec{r},t\right), \quad (1)$$

where $\phi(\vec{r},t)$ is the neutron flux ($cm^{-2}s^{-1}$), v is the neutron velocity (cm/s), $D\left(\phi(\vec{r},t),\vec{r},t\right)$ is the neutron diffusion coefficient (cm), $\Sigma_{a,m}(\vec{r},t)$ is the macroscopic absorption cross-section of m-th nuclide (cm^{-1}), $S\left(\phi(\vec{r},t),\vec{r},t\right)$ is the neutron source term ($cm^{-3}s^{-1}$).

The source term $S\left(\phi(\vec{r},t),\vec{r},t\right)$ represents neutron production from fission, depending on factors like neutron flux, macroscopic fission cross-section, and delayed neutron contributions. Mathematically, the source term is expressed as:

$$S\left(\phi(\vec{r},t),r,t\right)=\phi(\vec{r},t)\sum_l\nu_l\Sigma_{f,l}(\vec{r},t)+$$

$$+\sum_g\sum_p\lambda_{p,g}C_{p,g}(\vec{r},t), \quad (2)$$

where ν_l is the average number of neutrons produced per fission of l-th nuclide, $\Sigma_{f,l}(\vec{r},t)$ is the macroscopic fission cross-section of l-th nuclide, $\lambda_{p,g}$ is the decay constant and $C_{p,g}(\vec{r},t)$ is the concentration of the p-th delayed neutron precursor of g-th parent nuclide.

To simplify the numerical analysis, we assume a constant diffusion coefficient [32]

$$D=D\left(\phi(\vec{r},t),\vec{r},t\right)=0.02\,\text{cm} \quad (3)$$

throughout the medium. While this maintains reasonable accuracy, it may introduce some errors, particularly if the medium's properties vary significantly. Future research could involve incorporating spatially and time-dependent diffusion coefficients to refine the model and address discrepancies arising from changes in the medium's properties.

In this study, the UC_2 medium is modeled in cylindrical geometry, with the cylinder characterized by radius R and height H. We use cylindrical coordinates (ρ, θ, z) to describe the spatial distribution of neutrons, where ρ is the radial distance from the central axis, θ is the azimuthal angle, z is the axial coordinate.

Central symmetry is assumed, making neutron flux and related quantities independent of the azimuthal angle θ

$$\frac{\partial\phi(\rho,\theta,z,t)}{\partial\theta}=0. \quad (4)$$

This reduces the problem from three spatial dimensions to just radial distance ρ and axial position z, simplifying the neutron diffusion equation and making it easier to solve numerically.

Thus, the neutron diffusion equation to be solved in cylindrical geometry with central symmetry and constant diffusion coefficient is:

$$\frac{1}{v}\frac{\partial\phi(\rho,z,t)}{\partial t}=D\nabla^2\phi(\rho,z,t)-$$

$$-\phi(\rho,z,t)\sum_m\Sigma_{a,m}(\rho,z,t)+S\left(\phi(\rho,z,t),\rho,z,t\right), \quad (5)$$

where $\nabla^2=\frac{1}{\rho}\frac{\partial}{\partial\rho}\left(\rho\frac{\partial}{\partial\rho}\right)+\frac{\partial^2}{\partial z^2}$ is Laplacian in cylindrical geometry with central symmetry.

In this study, the evolution of nuclide concentrations is modeled using nuclide balance equations, accounting for neutron-induced reactions, beta decay, and transmutation. For any i-th nuclide, the general form of the balance equation is:

$$\frac{dN_i(\rho,z,t)}{dt}=-\sigma_{i,f}\phi(\rho,z,t)N_i(\rho,z,t)-$$

$$-\sigma_{i,c}\phi(\rho,z,t)N_i(\rho,z,t)+$$

$$+\sum_j\sigma_{j\to i}\phi(\rho,z,t)N_j(\rho,z,t)-\lambda_iN_i(\rho,z,t)+$$

$$+\sum_k\lambda_kN_k(\rho,z,t), \quad (6)$$

where $N_i(\rho,z,t)$ is the concentration of i-th nuclide (cm^{-3}), $\sigma_{i,f}$ is the microscopic fission cross-section of i-th nuclide (cm^2), $\sigma_{i,c}$ is the microscopic neutron capture cross-section of i-th nuclide (cm^2), $\sigma_{j\to i}$ is the microscopic cross-section for the transmutation of j-th nuclide into i-th nuclide, λ_i is the decay constant of i-th nuclide (s^{-1}), λ_k is the decay constant of k-th parent nuclide that decays into i-th, $N_k(\rho,z,t)$ is the concentration of the parent k-th parent nuclide.

The conversion of fertile ^{238}U to fissile ^{239}Pu is critical in sustaining a traveling wave of nuclear fission. The process involves neutron capture by ^{238}U and subsequent beta decay of ^{239}U and ^{239}Np. The full reaction chain is described below:

$$^{238}\text{U}+\text{n}\to{}^{239}\text{U}\xrightarrow{\beta^-}{}^{239}\text{Np}\xrightarrow{\beta^-}{}^{239}\text{Pu}. \quad (7)$$

In addition to ^{238}U, ^{235}U also plays an important role in the reactor, providing a fissile material for initiating fission. To enhance the accuracy of our

model, we incorporate delayed neutron precursors for both ^{235}U and ^{239}Pu, using a 6-group approach.

The eventual equations governing the evolution of the nuclides involved in the reaction chain (7), along with ^{235}U, are presented below:

$$\frac{dN_{\text{U-235}}}{dt} = -\sigma_{\text{U-235},f}\phi N_{\text{U-235}} - \sigma_{\text{U-235},c}\phi N_{\text{U-235}}, \quad (8)$$

$$\frac{dN_{\text{U-238}}}{dt} = -\sigma_{\text{U-238},c}\phi N_{\text{U-238}}, \quad (9)$$

$$\frac{dN_{\text{U-239}}}{dt} = \sigma_{\text{U-238},c}\phi N_{\text{U-238}} - \lambda_{\text{U-239}} N_{\text{U-239}}, \quad (10)$$

$$\frac{dN_{\text{Np-239}}}{dt} = \lambda_{\text{U-239}} N_{\text{U-239}} - \lambda_{\text{Np-239}} N_{\text{Np-239}}, \quad (11)$$

$$\frac{dN_{\text{Pu-239}}}{dt} = \lambda_{\text{Np-239}} N_{\text{Np-239}} - \\ -\sigma_{\text{Pu-239},f}\phi N_{\text{Pu-239}} - \sigma_{\text{Pu-239},c}\phi N_{\text{Pu-239}}. \quad (12)$$

Using a 6-group approach, we model delayed neutron precursors from the fission of ^{235}U and ^{239}Pu. Each *p*-th precursor of the *g*-th parent nuclide (^{235}U and ^{239}Pu) has its own decay constant $\lambda_{p,g}$ and delayed neutron fraction $\beta_{p,g}$.

The balance equation for the *p*-th delayed neutron precursor of the *g*-th parent nuclide is given by:

$$\frac{\partial C_{p,g}(\rho,z,t)}{\partial t} = \beta_{p,g}\sigma_{g,f}\phi(\rho,z,t) N_g(\rho,z,t) - \\ -\lambda_{p,g} C_{p,g}(\rho,z,t), \quad (13)$$

where $C_{p,g}(\rho,z,t)$ is the concentration of the *p*-th delayed neutron precursor of the *g*-th parent nuclide.

For the parent nuclide ^{235}U, the balanced equation for the *p*-th delayed neutron precursor is:

$$\frac{\partial C_{p,\text{U-235}}}{\partial t} = \beta_{p,\text{U-235}}\sigma_{\text{U-235},f}\phi N_{\text{U-235}} - \lambda_{p,\text{U-235}} C_{p,\text{U-235}}. \quad (14)$$

For the parent nuclide ^{239}Pu, the balance equation for the *p*-th delayed neutron precursor is:

$$\frac{\partial C_{p,\text{Pu-239}}}{\partial t} = \beta_{p,\text{Pu-239}}\sigma_{\text{Pu-239},f}\phi N_{\text{Pu-239}} - \lambda_{p,\text{Pu-239}} C_{p,\text{Pu-239}}. \quad (15)$$

The full system of equations – combining the neutron diffusion Eq. (5), nuclide balance Eqs. (8) - (12), and delayed neutron precursor Eqs. (14) and (15) – describes the evolution of neutron flux and nuclide concentrations in the UC_2 medium. Solving this system offers valuable insights into the propagation and stability of the traveling wave of nuclear fission.

3. Numerical model setup

The modeled system consists of a cylindrical fuel medium composed of UC_2. The cylinder is initially enriched with 15 % ^{235}U, while the remaining 85 % consists of ^{238}U. The fuel composition is treated as a homogeneous mixture of ^{235}U, ^{238}U, and carbon.

At the start of the simulation, the neutron flux within the medium is set to zero $\phi(\rho,z,t)\big|_{t=0} = 0$. To initiate the fission wave, a steady neutron current density of 10^{15} cm^{-2}s^{-1} is applied at one end of the cylinder (referred to as the injection base) for a duration long enough to allow the system to reach a self-sustaining state.

The boundary condition at the injection base for the neutron current density is:

$$J_0 = -D\frac{\partial\phi}{\partial z}\bigg|_{z=0} = 10^{15}\,\text{cm}^{-2}\text{s}^{-1}. \quad (16)$$

This high-intensity neutron source is necessary to generate sufficient ^{239}Pu through neutron capture by ^{238}U, enabling the fission wave to become self-sustaining after the source is removed.

Heat exchange is assumed to occur through the side surface of the cylinder and will be addressed in future work. For this surface, we introduce the concept of an abstract protective shell:

$$\frac{1}{\phi_R}\frac{\partial\phi}{\partial\rho}\bigg|_{\rho=R} = -\frac{1}{d}, \quad (17)$$

where *R* is the radius of the modeled cylinder and *d* is known as the extrapolated length. Conceptually, it separates the fissile medium from the coolant, allowing for simplification of the mathematical model while still accounting for neutron losses from the fissile medium.

The injection base, where the external neutron source is removed after initiation, is treated as a reflective boundary

$$\frac{\partial\phi}{\partial z}\bigg|_{z=0} = 0 \quad (18)$$

that prevents neutron leakage. Similarly, the opposite base (referred to as the termination base) of the cylinder, which does not interact with the neutron source, is also modeled as a reflector

$$\frac{\partial\phi}{\partial z}\bigg|_{z=H} = 0, \quad (19)$$

where *H* is the height of the modeled cylinder.

Table 1. **Key constants to model nuclide evolution**

Nuclide	Microscopic fission cross-section σ_f, b	Microscopic absorption cross-section σ_a, b	Decay constant λ, 1/s
^{235}U	136.43	57.61	–
^{238}U	–	252.5	–
^{239}U	–	4.8	$492.53 \cdot 10^{-6}$
^{239}Np	–	–	$3.4 \cdot 10^{-6}$
^{239}Pu	473.43	286.15	–

Table 2. **Key constants to model delayed neutron precursor evolution**

Delayed neutron precursor		Decay constant λ_p, s^{-1}	Delayed neutron fraction β_p
Parent nuclide	Number		
^{235}U	1	0.0124	0.000215
	2	0.0305	0.001424
	3	0.111	0.001274
	4	0.301	0.002568
	5	1.14	0.000748
	6	3.01	0.000273
^{239}Pu	1	0.01231	0.0000072
	2	0.03	0.000626
	3	0.12375	0.000444
	4	0.325352	0.000685
	5	1.117741	0.000180
	6	2.66538	0.000093

For the simulation, we employed specific microscopic cross-sections and decay constants for the key nuclides involved in the fission process, along with the decay constants and delayed neutron fractions for each precursor group associated with ^{235}U and ^{239}Pu, as presented in Tables 1 and 2, respectively, with values sourced from [32].

4. Numerical method

In this study, we use the control volume formulation (CVF) to numerically solve the neutron diffusion equation in a cylindrical UC_2 medium. CVF discretizes the domain into finite control volumes and integrates the governing equations over each, resulting in algebraic equations that approximate the original partial differential equations. By applying finite differences for flux and its derivatives, CVF efficiently solves for the neutron flux distribution $\phi(\rho,z,t)$. This method is particularly effective for conservation laws like neutron diffusion.

The neutron diffusion equation is integrated over the control volume of the node ($\rho_j = j\Delta\rho$, $z_k = k\Delta z$) and over the time interval from t_i to $t_{i+1} = t_i + \Delta t$:

$$\frac{1}{\nu}\int_{t_i}^{t_{i+1}}\int_{z_{k-\frac{1}{2}}}^{z_{k+\frac{1}{2}}}\int_{\rho_{j-\frac{1}{2}}}^{\rho_{j+\frac{1}{2}}}\rho\frac{\partial\phi(\rho,z,t)}{\partial t}d\rho dzdt = D\int_{t_i}^{t_{i+1}}\int_{z_{k-\frac{1}{2}}}^{z_{k+\frac{1}{2}}}\int_{\rho_{j-\frac{1}{2}}}^{\rho_{j+\frac{1}{2}}}\rho\left[\frac{1}{\rho}\frac{\partial}{\partial\rho}\left(\rho\frac{\partial\phi(\rho,z,t)}{\partial\rho}\right)+\frac{\partial^2\phi(\rho,z,t)}{\partial z^2}\right]d\rho dzdt -$$

$$-\int_{t_i}^{t_{i+1}}\int_{z_{k-\frac{1}{2}}}^{z_{k+\frac{1}{2}}}\int_{\rho_{j-\frac{1}{2}}}^{\rho_{j+\frac{1}{2}}}\rho\phi(\rho,z,t)\sum\nolimits_m\Sigma_{a,m}(\rho,z,t)d\rho dzdt+\int_{t_i}^{t_{i+1}}\int_{z_{k-\frac{1}{2}}}^{z_{k+\frac{1}{2}}}\int_{\rho_{j-\frac{1}{2}}}^{\rho_{j+\frac{1}{2}}}\rho S\left(\phi(\rho,z,t),\rho,z,t\right)d\rho dzdt, \qquad (20)$$

where the integral of the source term is

$$\int_{t_i}^{t_{i+1}}\int_{z_{k-\frac{1}{2}}}^{z_{k+\frac{1}{2}}}\int_{\rho_{j-\frac{1}{2}}}^{\rho_{j+\frac{1}{2}}}\rho S\left(\phi(\rho,z,t),\rho,z,t\right)d\rho dzdt = \int_{t_i}^{t_{i+1}}\int_{z_{k-\frac{1}{2}}}^{z_{k+\frac{1}{2}}}\int_{\rho_{j-\frac{1}{2}}}^{\rho_{j+\frac{1}{2}}}\rho\phi(\rho,z,t)\sum\nolimits_l\nu_l\Sigma_{f,l}(\rho,z,t)d\rho dzdt +$$

$$+\sum\nolimits_g\sum\nolimits_p\lambda_{p,g}\int_{t_i}^{t_{i+1}}\int_{z_{k-\frac{1}{2}}}^{z_{k+\frac{1}{2}}}\int_{\rho_{j-\frac{1}{2}}}^{\rho_{j+\frac{1}{2}}}\rho C_{p,g}(\rho,z,t)d\rho dzdt. \qquad (21)$$

We approximate the integral (20) using the following discrete analog:

$$-a^{\rho}_{i,j,k}\phi^{i+1}_{j-1,k}+b_{i,j,k}\phi^{i+1}_{j,k}-c^{\rho}_{i,j,k}\phi^{i+1}_{j+1,k}=d^{\rho}_{i,j,k}, \quad (22)$$

where

$$b_{i,j,k}=j\Delta\rho^2\Delta z+2\,jD\Delta t\Delta z+2\frac{Dj\Delta\rho^2\Delta t}{\Delta z}+j\Delta\rho^2\Delta z\Delta t\sum\nolimits_m\Sigma^{i,j,k}_{a,m}, \quad (23)$$

$$a^{\rho}_{i,j,k}=D\Delta t\Delta z\left(j-\frac{1}{2}\right), \quad (24)$$

$$c^{\rho}_{i,j,k}=D\Delta t\Delta z\left(j+\frac{1}{2}\right), \quad (25)$$

$$a^{z}_{i,j,k}=\frac{Dj\Delta\rho^2\Delta t}{\Delta z}, \quad (26)$$

$$\bar{b}_{i,j,k}=j\Delta\rho^2\Delta z+j\Delta\rho^2\Delta z\Delta t\sum\nolimits_l\upsilon_l\Sigma^{i,j,k}_{f,l}, \quad (27)$$

$$\bar{c}^{z}_{i,j,k}=\frac{Dj\Delta\rho^2\Delta t}{\Delta z}, \quad (28)$$

$$d^{\rho}_{i,j,k}=a^{z}_{i,j,k}\phi^{i+1}_{j,k-1}+\bar{b}_{i,j,k}\phi^{i}_{j,k}+\bar{c}^{z}_{i,j,k}\phi^{i}_{j,k+1}+d_{i,j,k}, \quad (29)$$

$$d_{i,j,k}=j\Delta\rho^2\Delta z\Delta t\sum\nolimits_g\sum\nolimits_p\lambda_{p,g}C^{i,j,k}_{p,g}. \quad (30)$$

With the discrete analog (22), we form a tridiagonal system of algebraic equations, which in matrix form is represented as:

$$\begin{bmatrix} b_{i,0,k} & -c^{\rho}_{i,0,k} & 0 & \cdots & 0 & 0 & 0 \\ -a^{\rho}_{i,1,k} & b_{i,1,k} & -c^{\rho}_{i,1,k} & \ldots & 0 & 0 & 0 \\ \vdots & \ddots & \ddots & \ddots & \ddots & \ddots & \vdots \\ 0 & \ldots & -a^{\rho}_{i,j,k} & b_{i,j,k} & -c^{\rho}_{i,j,k} & \ldots & 0 \\ \vdots & \ddots & \ddots & \ddots & \ddots & \ddots & \vdots \\ 0 & 0 & 0 & \ldots & -a^{\rho}_{i,N_R-1,k} & b_{i,N_R-1,k} & -c^{\rho}_{i,N_R-1,k} \\ 0 & 0 & 0 & \ldots & 0 & -a^{\rho}_{i,N_R,k} & b_{i,N_R,k} \end{bmatrix} \begin{bmatrix} \phi^{i+1}_{0,k} \\ \phi^{i+1}_{1,k} \\ \vdots \\ \phi^{i+1}_{j,k} \\ \vdots \\ \phi^{i+1}_{N_R-1,k} \\ \phi^{i+1}_{N_R,k} \end{bmatrix} = \begin{bmatrix} d^{\rho}_{i,0,k} \\ d^{\rho}_{i,1,k} \\ \vdots \\ d^{\rho}_{i,j,k} \\ \vdots \\ d^{\rho}_{i,N_R-1,k} \\ d^{\rho}_{i,N_R,k} \end{bmatrix} \quad (31)$$

for each *k*-th layer of the cylinder along *Oz*-axis. This allows for an efficient numerical solution, as tridiagonal systems can be solved using specialized algorithms such as the Thomas algorithm, which reduces computational complexity. The solution for each *k*-layer is sequentially obtained based on the results from the previous (*k*-1)-layer, ensuring that the propagation of the traveling wave of nuclear fission is accurately modeled.

The numerical solution for the nuclide balance equation can be achieved more easily than for neutrons, but it provides an important criterion for selecting the time step Δ*t*. A first-order Taylor approximation is applied:

$$N\left(\rho_j,z_k,t_{i+1}\right)=N^{i+1}_{j,k}=N^{i}_{j,k}+\frac{\partial \mathrm{N}}{\partial \mathrm{t}}\bigg|_{\substack{\rho=\rho_j\\ z=z_k\\ t=t_i}}\Delta t. \quad (32)$$

By demanding that calculated concentrations remain non-negative $N^{i}_{j,k}+\frac{\partial N}{\partial t}\Big|_{\substack{\rho=\rho_j\\ z=z_k\\ t=t_i}}\Delta t\geq 0$, we derive the following criterion for the time step:

$$\Delta t\geq -N^{i}_{j,k}\Big/\frac{\partial N}{\partial t}\bigg|_{\substack{\rho=\rho_j\\ z=z_k\\ t=t_i}}. \quad (33)$$

5. Results and discussion

In this section, we present the results of our 3D numerical simulations of the traveling wave of nuclear fission, focusing on its propagation characteristics and dynamics. The Figures below demonstrate how key quantities within the medium evolve over time, providing valuable insights into the stability and fuel efficiency of the TWR.

Two numerical experiments were conducted: the first as an initial trial and the second with more detailed settings, as outlined in Table 3.

Table 3. **Simulation parameters for numerical experiments**

Parameter	Experiment 1	Experiment 2
Diameter	10 cm	
Height	15 cm	20 cm
Radial step	1 mm	
Axial step	1 cm	1 mm
Time step	0.1 s	
External source duration	20 days	10 days

In Experiment 1, a larger axial step size Δz - 1 cm was used. The results demonstrated a self-sustaining traveling wave of nuclear fission, with fluctuations observed at approximately 5-day intervals, linked to the accumulation and subsequent rapid burnout of ^{239}Pu.

Experiment 2 was conducted using a 10-times smaller axial step Δz - 1 mm, resulting in more accurate data. A self-sustaining traveling wave of nuclear fission was observed. Shortly after formation, the wave stabilized and became steady, with no fluctuations detected (Figs. 1 - 4). The wave's propagation velocity is approximately 2 - 3 mm/day, or around 1 m/year, with a fission front width of about 2 cm.

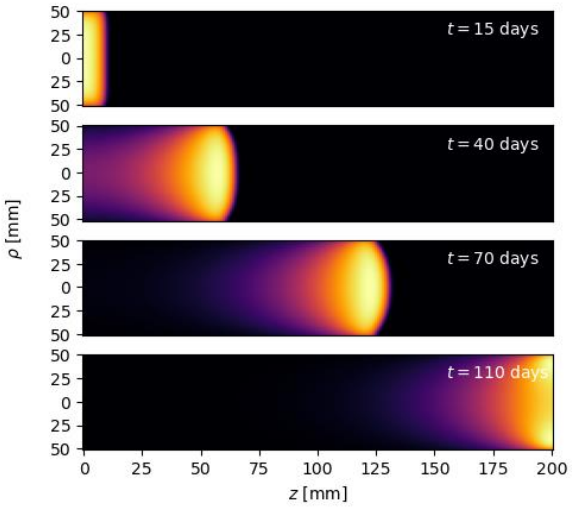

Fig. 1. 2D neutron dynamics along the central cross-section of the cylinder in Experiment 2. (See color Figure on the journal website.)

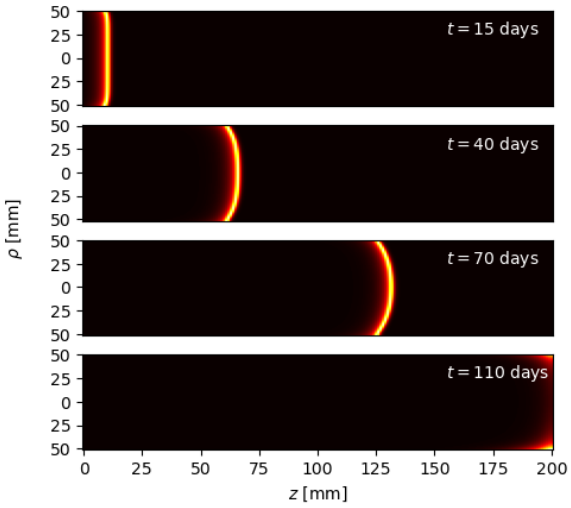

Fig. 2. 2D ^{239}Pu dynamics along the central cross-section of the cylinder in Experiment 2. (See color Figure on the journal website.)

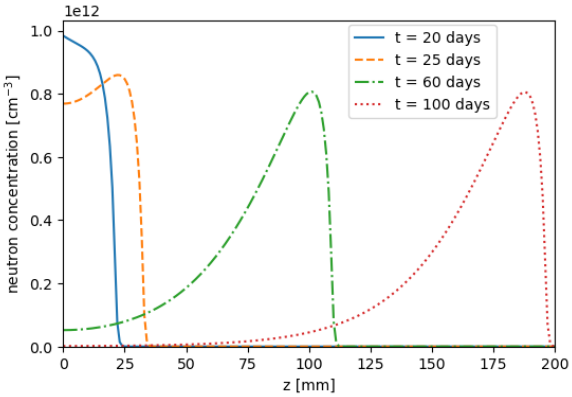

Fig. 3. Neutron propagation along the central axis (ρ = 0) of the cylinder in Experiment 2. (See color Figure on the journal website.)

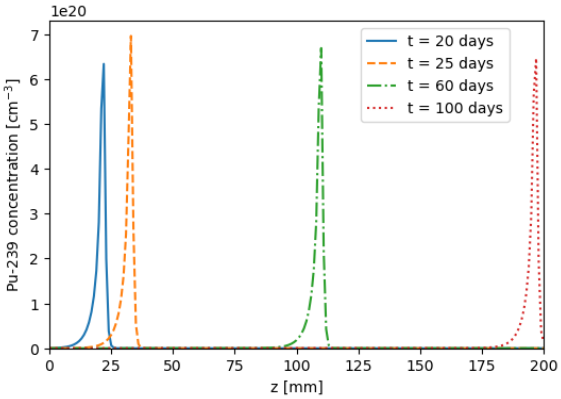

Fig. 4. ^{239}Pu propagation along the central axis (ρ = 0) of the cylinder in Experiment 2. (See color Figure on the journal website.)

It is clear that the larger axial step size of 1 cm is too coarse for modeling processes with parameters on the scale of 1 cm or smaller. A finer axial step, around 0.1 mm, would be more appropriate, though it would require significant computational resources.

The power generated by the self-sustaining traveling wave of nuclear fission in UC_2 was monitored throughout the simulation. Fig. 5 shows the power as a function of time, illustrating an initial rise during the early phase of fission wave propagation, with the power peaking at approximately 140 MW. After this peak, the power output stabilized, indicating the onset of a steady-state regime where the fission wave continued to propagate at a constant rate, sustaining the nuclear reaction without significant fluctuations, as long as fertile material remained available.

Further research is needed to explore heat transfer and material behavior under these conditions of such high-power production. Nevertheless, the high-power output is a promising result, positioning TWRs as a highly competitive option in advanced nuclear reactors.

As shown in Fig. 5, once the fission wave is formed, the burnout of ^{239}Pu begins to play the dominant role in energy production, contributing 100 MW compared to approximately 40 MW from ^{235}U. In Fig. 6, we can observe that once the fission wave stabilizes, ^{239}Pu produces roughly 2.5 times more neutrons than ^{235}U, which was initially used for enrichment to facilitate wave formation and further propagation.

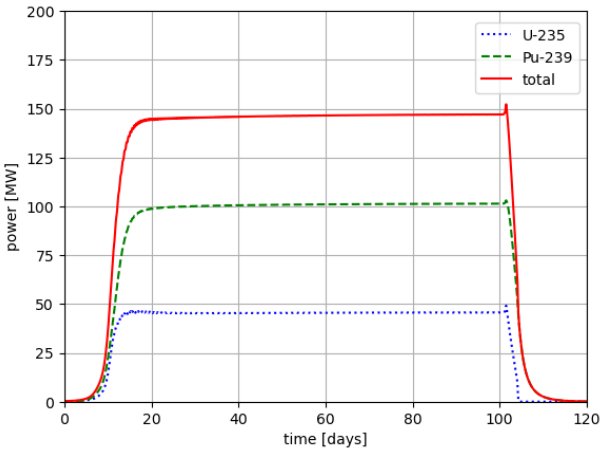

Fig. 5. Power output during fission wave propagation. (See color Figure on the journal website.)

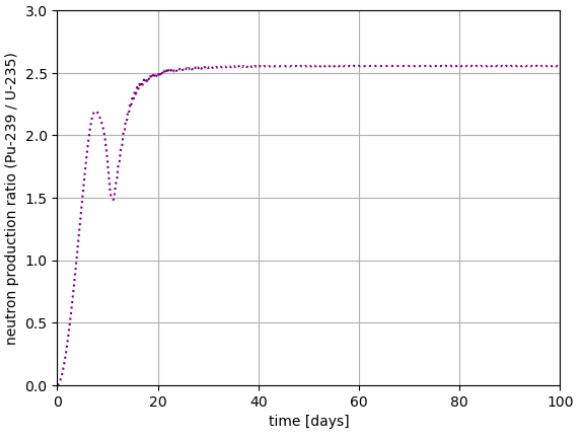

Fig. 6. Neutron production ratio of ^{239}Pu to ^{235}U during fission wave propagation. (See color Figure on the journal website.)

Although a high enrichment level of 15 % was applied in our initial simulations, the fission of ^{239}Pu still dominates the propagation of the nuclear fission wave through the UC_2 medium (Figs. 5 and 6). This suggests that the initial enrichment could potentially be lowered, possibly even to depleted uranium levels. However, further research is needed to determine the optimal conditions. Additionally, now that we understand the properties of a steady fission wave and the conditions required for its propagation, we can prepare a startup zone to make the process self-sustaining as quickly as possible, minimizing the need for a powerful external neutron source.

6. Conclusions

In this work, we presented the methodology and results of 3D numerical simulations of a traveling wave of nuclear fission in a cylindrical UC_2 medium. Given that many nuclear reactors are designed with cylindrical symmetry, this model is highly relevant for practical applications. We report, for the first time, results from a numerical experiment where the external neutron source was turned off after the formation of a stable, self-sustaining traveling wave.

By employing the CVF, we achieved a robust numerical solution to the neutron diffusion equation, offering valuable insights into the propagation and stability of these waves in the UC_2 medium.

The simulations demonstrated significant nuclide burnout and efficient power production, meeting key criteria expected for TWRs, including fuel efficiency, waste reduction, resistance to nuclear proliferation, and enhanced safety.

While the current model is simplified – focusing solely on the active zone and excluding structural materials, moderators, and coolant – it provides a solid foundation for further development. Future research will enhance the model by incorporating additional nuclides interacting with neutrons and extending the neutron diffusion equation to include specific coolants and protective shells. This iterative approach ensures steady progress toward a comprehensive and realistic model.

REFERENCES

1. L.P. Feoktistov. Neutron-fission wave. Doklady Akademii Nauk SSSR 309 (1989) 864. (Rus)
2. L.P. Feoktistov. Safety is key to the revival of nuclear power. Uspekhi Fizicheskikh Nauk 163(8) (1993) 89. (Rus)
3. E. Teller et al. Completely automated nuclear reactors for long-term operation II: Toward a concept-level point-design of a high-temperature, gas-cooled central power station system. Part II. In: Proceedings of the International Conference on Emerging Nuclear Energy Systems (ICENES'96), Obninsk, Russian Federation, 1996, p. 123.
4. V.Ya. Goldin, D.Yu. Anistratov. Fast neutron reactor in a self-regulating neutron-nuclear mode. Matematicheskoye Modelirovaniye 7(10) (1995) 12. (Rus)
5. V.Ya. Goldin, N.V. Sosnin, Yu.V. Troschiev. Fast reactor in self-regulation mode of the 2nd kind. Doklady Rossiyskoy Akademii Nauk, Matematicheskaya Fizika 358(6) (1998) 747. (Rus)
6. A.I. Akhiezer et al. On the theory of propagation of chain nuclear reaction in diffusion approximation. Yadernaya Fizika 62 (1999) 1567. (Rus)
7. H. Sekimoto, K. Ryu, Y. Yoshimura. CANDLE: The new burnup strategy. Nuclear Science and Engineering 139 (2001) 306.
8. H. Sekimoto, K. Ryu. A new reactor burnup concept "CANDLE." In: Proceeding of PHYSOR 2000, Pittsburgh, May 7-11, 2000.
9. V.D. Rusov et al. Geoantineutrino spectrum and slow nuclear burning on the boundary of the liquid and solid phases of the Earth's core. arXiv:hep-ph/0402039 (2004).
10. V.D. Rusov et al. Geoantineutrino spectrum and slow nuclear burning on the boundary of the liquid and

solid phases of the Earth's core. J. Geophys. Res. 112 (2007) B09203.
11. S.P. Fomin et al. Study of self-organizing regime of nuclear burning wave in fast reactor. Problems of Atomic Science and Technology 6(45) (2005) 106.
12. S. Fomin et al. Self-sustained regime of nuclear burning wave in U-Pu fast reactor with Pb-Bi coolant. Problems of Atomic Science and Technology 3(1) (2007) 156.
13. N. Takaki, H. Sekimoto. Potential of CANDLE Reactor on Sustainable Development and Strengthened Proliferation Resistance. Prog. Nucl. Energy 50 (2008) 114.
14. J. Gilleland et al. Novel reactor designs to burn non-fissile fuels. In: Proceedings of the International Conference on Advances in Nuclear Power Plants (ICAPP 2008), Anaheim, CA, USA, June 8 - 12, 2008, p. 2278.
15. K.D. Weaver et al. A Once-Through Fuel Cycle for Fast Reactors. J. Eng. Gas Turbines and Power 132 (2010) 102917.
16. T. Ellis et al. Traveling-wave reactors: A truly sustainable and full-scale resource for global energy needs. In: Proceedings of the International Congress on Advances in Nuclear Power Plants (ICAPP 2010), San Diego, CA, USA, June 13 - 17, 2010, Paper No. 10189.
17. C.E. Ahlfeld et al. Traveling wave nuclear fission reactor, fuel assembly, and method of controlling burnup therein. Patent No.: US 8942338 B2. Date of Patent: Jan. 27, 2015.
18. X.-N. Chen, W. Maschek. Transverse buckling effects on solitary burn-up waves. Annals of Nuclear Energy 32 (2005) 1377.
19. V.D. Rusov et al. Traveling wave reactor and condition of existence of nuclear burning soliton-like wave in neutron-multiplying media. Energies 4(9) (2011) 1337.
20. X.-N. Chen et al. Fundamental solution of nuclear solitary wave. Energy Conversion and Management 59 (2012) 40.
21. A.G. Osborne, M.R. Deinert. Neutron damage reduction in a traveling wave reactor. In: Proceedings of the Conference on Advances in Reactor Physics (PHYSOR 2012), Knoxville, TN, USA, April 15 - 20, 2012.
22. V.D. Rusov et al. *Traveling Wave Nuclear Reactor* (Kyiv: Publishing group "A.C.C.", 2013) 156 p. (Rus)
23. A.G. Osborne, M.R. Deinert. Comparison of neutron diffusion and Monte Carlo simulations of a fission wave. Annals of Nuclear Energy 62 (2013) 269.
24. V.D. Rusov et al. On some fundamental peculiarities of the traveling wave reactor. Science and Technology of Nuclear Installations (2015) 703069.
25. S. Qvist, J. Hou, E. Greenspan. Design and performance of 2D and 3D-shuffled breed-and-burn cores. Annals of Nuclear Energy 85 (2015) 93.
26. J. Hou et al. 3D in-core fuel management optimization for breed-and-burn reactors. Progress in Nuclear Energy 88 (2016) 58.
27. V.M. Khotyayintsev, V.M. Pavlovych, O.M. Khotyayintseva. Travelling-wave reactor: velocity formation mechanisms. In: Proceedings of the International Conference on the Physics of Reactors: Advances in Reactor Physics to Power the Nuclear Renaissance (PHYSOR 2010), Pittsburgh, PA, USA, May 9-14, 2010.
28. V.M. Khotyayintsev et al. Velocity characteristic and stability of wave solutions for a CANDLE reactor with thermal feedback. Annals of Nuclear Energy 85 (2015) 337.
29. O.M. Khotyayintseva V.M. Khotyayintsev, V.M. Pavlovych. Reactivity in the theory of stationary nuclear fission wave. Nucl. Phys. At. Energy 17(2) (2016) 157. (Ukr)
30. V.D. Rusov et al. Fast traveling-wave reactor of the channel type. Interdisciplinary Studies of Complex Systems 9 (2017) 36.
31. S.P. Fomin et al. Influence of the radial neutron reflector efficiency on the power of fast nuclear-burning-wave reactor. Annals of Nuclear Energy 148 (2020) 107699.
32. V.D. Rusov et al. Ultraslow wave nuclear burning of uranium-plutonium fissile medium on epithermal neutrons. Progress in Nuclear Energy 83 (2015) 105.
33. D. Ray et al. Build-up and characterization of ultra-slow nuclear burnup wave in epithermal neutron multiplying medium. ASME J. of Nucl. Rad. Sci. 8(2) (2022) 021501.
34. A.E. Pomysukhina, Yu.P. Sukharev, G.N. Vlasichev. Reactor based on nuclear burning wave in U-Th fuel cycle. Trudy Nizhegorodskogo Gosudarstvennogo Tekhnicheskogo Universiteta (Proceedings of Nizhny Novgorod State Technical University) 2(125) (2019) 136. (Rus)
35. A.O. Kakaev et al. Simulation of the nuclear burning wave of ^{232}Th in the ^{239}Pu enrichment for the neutron energy thermal area. Journal of Physical Studies 24(1) (2020) 1201.
36. M.R. Shcherbyna, V.O. Tarasov, V.P. Smolyar. Wave nuclear burning in spherical geometry. Journal of Physical Studies 25(2) (2021) 2202.
37. V. Tarasov et al. Simulation of the traveling wave burning regime on epithermal neutrons. World Journal of Nuclear Science and Technology 13(4) (2023) 73.
38. V.D. Rusov et al. Neutron moderation theory with thermal motion of the moderator nuclei. The European Physical Journal A 53 (2017) 179.
39. V.P. Smolyar et al. Geant4 simulation of the moderating neutrons spectrum. Radiation Physics and Chemistry 212 (2023) 111151.
40. V.L. Aksenov et al. On the limit of neutron fluxes in the fission-based pulsed neutron sources. Phys. Part. Nucl. Lett. 14(5) (2017) 788.
41. E.P. Shabalin et al. High-intensity pulsed neutron research reactor based on neptunium. Preprint JINR P13-2017-57 (Dubna, 2017) 18 p.
42. A.V. Arapov et al. Results of the physical start-up of the BR-1M reactor. In: Problems of High Energy Density Physics. XII Kharitonov Thematic Scientific Readings. Reports (Sarov: Publishing House "Russian Federal Nuclear Center - All-Russian Research Institute of Experimental Physics", 2010) 553 p.

**М. Р. Щербина*, К. О. Щербина, В. О. Тарасов,
С. І. Косенко, С. А. Чернеженко**

Національний університет «Одеська політехніка», Одеса, Україна

*Відповідальний автор: mykhailo.shcherbyna@yahoo.com

ЧИСЛОВИЙ АНАЛІЗ САМОЖИВИЛЬНОЇ РУХОМОЇ ХВИЛІ ЯДЕРНОГО ПОДІЛУ, ПРОПАГОВАНОЇ НАДТЕПЛОВИМИ НЕЙТРОНАМИ В СЕРЕДОВИЩІ УРАНУ ДІКАРБІДУ

Досліджено саможивильну рухому хвилю ядерного поділу в середовищі урану дікарбіду через чисельне розв’язання системи диференціальних рівнянь. Основна увага приділяється рівнянню дифузії нейтронів та рівнянням балансу нуклідів, які є ключовими для розуміння поведінки хвиль поділу. Метою дослідження є визначення характеристик поширення та перевірка стабільності хвиль ядерного поділу. Числовий аналіз надає глибокі уявлення про динаміку розподілу нейтронів та зміну нуклідного складу, що є корисним у проєктуванні реакторів рухомої хвилі ядерного поділу.

Ключові слова: реактор рухомої хвилі ядерного поділу, надтеплові нейтрони, уран дікарбід, рівняння дифузії нейтронів, конструкція реактора, саможивильна хвиля поділу.

Надійшла / Received 03.10.2024